

REITERATIVE DOMAIN AWARE MULTI-TARGET ADAPTATION

Sudipan Saha¹, Shan Zhao¹, Nasrullah Sheikh², Xiao Xiang Zhu^{1,3}

Technical University of Munich, Taufkirchen/Ottobrunn, Germany¹

IBM Research Almaden, CA, USA ²

German Aerospace Center (DLR), Weßling, Germany³

ABSTRACT

Most domain adaptation methods focus on single-source-single-target adaptation settings. Multi-target domain adaptation is a powerful extension in which a single classifier is learned for multiple unlabeled target domains. To build a multi-target classifier, it is important to have: a feature extractor that generalizes well across domains; and effective aggregation of features from the labeled source and different unlabeled target domains. Towards the first, we use the recently popular Transformer as a feature extraction backbone. Towards the second, we use a co-teaching-based approach using a dual-classifier head, one of which is based on the graph neural network. The proposed approach uses a sequential adaptation strategy that adapts one domain at a time starting from the target domains that are more similar to the source, assuming that the network finds it easier to adapt to such target domains. After adapting on each target, samples with a softmax-based confidence score greater than a threshold are added to the pseudo-source, thus aggregating knowledge from different domains. However, softmax is not entirely trustworthy as a confidence score and may generate a high score for unreliable samples if trained for many iterations. To mitigate this effect, we adopt a reiterative approach, where we reduce target adaptation iterations, however, reiterate multiple times over the target domains. The experimental evaluation on the Office-Home, Office-31 and DomainNet datasets shows significant improvement over the existing methods. We have achieved 10.7% average improvement in Office-Home dataset over the state-of-art methods.

1. INTRODUCTION

The deep learning techniques have produced an impressive performance for a wide array of visual inference tasks [1, 2, 3, 4, 5]. Yet, these models fail to generalize when exposed to a new environment. This is caused by a misalignment between the source and the target data distributions, causing the trained model to perform poorly during inference [6]. Since collecting labeled data for each domain is challenging, a rich line of research, unsupervised domain adaptation [7, 8], has evolved to effectively exploit the source data to learn a robust classifier on the target domain(s).

Most domain adaptation methods are designed to adapt to a single unlabeled target from a single labeled source domain. Such methods include those based on generative modeling [9, 10], adversarial training [11], and statistical alignment [12, 13, 14]. However, such models are not suitable for practical settings where we may come across many target domains as a separate model needs to be trained for each target domain. Recently, some works in the literature have addressed this issue by designing methods to adapt to multiple domains simultaneously from a single source domain [15]. This domain adaptation setting is called Multi-target Domain Adaptation (MTDA). MTDA methods can be both domain-agnostic/aware, depending on the availability of the domain labels of target samples [16].

MTDA is challenging as the increase of the domains brings more difficulty in aligning feature distributions among them. While previous works focus on merely aligning cross-domain distributions [16], the generalization ability of the backbone feature extractor may play a crucial role in multi-target adaptation. Transformers have recently shown excellent capability in many computer vision tasks [17]. Unlike CNN which generally concentrates on the local features, the Vision Transformer (ViT) [18] exploits the attention across the patches to capture the long-distance features and acquires global information. Moreover, Transformer-based models have shown good performance in transfer learning and domain adaptation [19, 20, 21]. Motivated by this, we propose to use pre-trained Transformer as a feature extractor for MTDA. We hypothesize that the strong generalization capability of Transformer-based features will enhance the adaptation ability across multiple target domains.

Furthermore, to learn an effective multi-target classifier, it may be useful to aggregate features from different domains. To this end, graph neural networks (GNNs) have been found to be effective [22]. By exploiting GNN's potential in tandem with co-teaching and curriculum learning, Roy *et. al.* [16] proposed Domain-aware Curriculum Graph Co-Teaching (DCGCT) for MTDA. Curriculum learning is a type of learning in which easy examples are tackled first while gradually increasing the task difficulty [23, 24]. Inspired by this, we adopt this paradigm in conjunction with Transformer-based feature extraction. Similar to [16], we use a dual classifier

comprising of a MLP head and a GNN head. One target domain is processed at a time, starting from the easiest domain or the domain closest to the source domain. Minibatches comprising of source samples and target samples are fed to the dual-head classifier. While the MLP based classifier focuses on the individual samples, the GNN based classifier aggregates features from different samples in the minibatch. Similar to co-teaching [25], they help each other in an iterative manner to learn effective target classifier. The pseudo-labels are selected after processing each domain and are used along with the source domain samples for processing the following target domains. The crux of the idea is that pseudo-labeled samples (henceforth called pseudo-samples) from the easier domains assist in adapting the classifier on the more difficult target domains. One caveat of this idea is that it is not trivial to select pseudo-samples from the target domains. In [16], a simple strategy based on softmax score is used. After adapting on a target domain, the target samples exceeding a threshold softmax value are selected as pseudo-labeled samples. However, softmax is not a reliable confidence indicator for deep learning models [26, 27] and may yield overconfident predictions if trained for the high number of training iterations. Reducing the number of training iterations over a target domain may lead to the selection of the higher quality, however lesser number of pseudo samples. To compensate lesser pseudo samples selected in one training cycle, we postulate that the MLP-GNN dual classifier can be better adapted to target domains by reiterating multiple times over the set of target domains. Pseudo-source is initialized with the source samples and ingests some target pseudo-samples after each reiteration. In practice, the total number of training iterations is conserved as in D-CGCT.

In contrast to D-CGCT [16], we use more source samples than target samples in each minibatch during training. Even though our goal is to adapt the classifier on the target domains, the primary reference of guidance for the classifier is the labeled source samples. Hence we postulate that more source samples in comparison to the target samples in a minibatch can improve the adaptation performance.

The contributions of this work are as follows:

1. We introduce Transformer in the context of multi-target adaptation.
2. We combine Transformer and GNN in the same framework to obtain a superior MTDA framework that benefits simultaneously from the excellent generalization ability of the Transformer backbone and feature aggregation capability of GNN.
3. We furthermore show that by choosing more source samples than target samples in the training minibatch improves MTDA performance.
4. We experimentally validate on three popular benchmark datasets showing a significant improvement over

the existing domain-aware MTDA frameworks, e.g., 10.7% average improvement over D-CGCT in Office-Home dataset.

2. RELATED WORKS

Mitigating the discrepancy between the training and test data distributions is a long lasting problem. The machine learning and computer vision literature is rich in domain adaptation techniques for several problems including image classification, semantic segmentation, and object recognition [6]. In this regard, domain adaptation aligns the data distribution using generative modeling [9, 10], adversarial training [11, 28], and standard divergence measures [13, 14]. The domain adaptation problem can be presented in various flavors depending on the overlap of classes between domains (closed-set, open-set) [29, 30, 31] or number of sources and targets, e.g., single-source-single-target, multi-source [32, 33, 34], multi-target [35, 36, 37].

Multi-target domain adaptation [16, 35, 38, 36, 39, 15] transfers a network learned on a single labeled source dataset to multiple unlabeled target datasets. This line of research is quite new and there are only few methods towards this direction. While there has been extensive research on single-target domain adaptation, those methods cannot be trivially applied in the multi-target setting. The method in [39] clusters the blended target domain samples to obtain sub-targets and subsequently applies a single-target domain adaptation method on the source and the obtained sub-targets. Multi-teacher MTDA (MT-MTDA) [15] uses knowledge distillation to distill target domain knowledge from multiple teachers to a common student.

Sequentially adapting the source classifier to each target domain for multi-target adaptation is related to incremental learning. Incremental learning [40] continually trains a classifier for sequentially available data for novel tasks. There are only few existing works in the domain adaptation literature [41, 42] in this line.

Learning from noisy labels is an important topic in weakly supervised learning. A recently popular approach to handle noisy labels is co-teaching [25] that cross-trains two deep networks that teach each other given every minibatch. While the predictions from the two classifiers may strongly disagree at the beginning, the two networks converge towards consensus with the increase of training epochs.

Graph Neural Networks (GNNs) are neural networks applied on the graph-structured data. GNNs can capture the relationships between the nodes (objects) in a graph using the edges [43]. GNNs [43] have been recently adopted for progressive/incremental domain adaptation [44, 16]. Progressive Graph Learning (PGL) [44] operates in single-target setting where a graph neural network with episodic training is integrated to suppress the underlying conditional shift and to close the gap between the source and target distributions.

Further extending this concept, [16] proposes a method for multi-target domain adaptation. As discussed in Section 1, our method is closely related to [16]. While their method is applicable to both domain-agnostic and domain-aware setting, in our work we focus on the domain-aware setting in [16], i.e., D-CGCT. A heterogeneous Graph Attention Network (HGAN) is used for MTDA in [38].

Transformer is a recently popular deep learning architecture. The fundamental building block of a Transformer is self-attention. Attention mechanism computes the responses at each token in a sequence by attending it to all tokens and gathering the corresponding embeddings based on the attention scores accordingly [17]. To extend the application of Transformer to the grid-like data, ViT is proposed, which uses a pure Transformer and formulates the classification problem as a sequential problem by splitting the image into a sequence of patches. It is composed of three main components: a linear layer to project flattened image patches to lower dimensional embeddings, the standard Transformer encoder with multi-head self-attention to compute independent scoring functions from different subspaces, and a MLP head for classification score prediction. Different variants of image-based have been proposed, e.g., Data-efficient image Transformers (DeiT) [45], Convolutional vision Transformer (CvT) [46], Compact Convolutional Transformer (CCT) [47], and LocalViT [48]. Recently the application of Transformers in computer vision tasks including image generation [49], object detection [50], classification and segmentation [51] has sprung up due to its advantageous capability. The Transformer encoder in ViTs can be regarded as a feature extractor naturally. Unlike CNN which merely concentrates on local features, the attention across the patches captures the long distance features and acquires global information. Transformers have shown good performance in transfer learning [19], e.g. in medical image analysis [20]. Furthermore, Transformers have been shown to be useful for source-free domain adaptation in [21]. They make the observation that focusing attention on the objects in the image plays an important role in domain adaptation.

Similar to [21], our work exploits Transformer as backbone feature extractor to capitalize on its ability to generalize across domains. MTDA is a relatively new area, where our work is related to [16]. However, in contrast to [16], we use a reiterative approach to effectively ingest target domain pseudo-samples. The learning of the dual-classifier head is based on co-teaching [25] and follows similar episodic training as in [44].

3. PROPOSED METHOD

For the proposed multi-target domain adaptation, we are provided with a source dataset \mathcal{S} containing n_s labeled samples $(\mathbf{x}_{s,i}, y_{s,i})_{i=1}^{n_s}$ and N target datasets $\mathcal{T} = \{\mathcal{T}_j\}_{j=1}^N$. The underlying data distributions of the source and the N target domains are different from each other. However, they share the

Algorithm 1: Proposed training procedure

require: number of target domains N , classes n_c
require: source dataset \mathcal{S} ; target dataset $\mathcal{T} = \{\mathcal{T}_j\}_{j=1}^N$
require: hyper-parameters B, τ, K, K^* ,
 $K', \lambda_{edge}, \lambda_{node}, \lambda_{adv}$
require: networks $F, D, G_{mlp}, f_{edge}, f_{node}$ with
parameters $\theta, \psi, \phi, \varphi, \varphi'$, respectively. The f_{edge}
and f_{node} form the G_{gnn} .

Step 1: Training on the source dataset

1 **while** ℓ_{ce} has not converged **do**
2 $(\mathbf{x}_{s,i}, y_{s,i})_{i=1}^{B_s} \sim \mathcal{S}$
3 update θ, ϕ by $\min_{\theta, \phi} \ell_{ce}^{mlp}$
4 **end**

Step 2: Curriculum learning

5 $\hat{\mathcal{S}}^{total} \leftarrow \mathcal{S}$ ▷ Pseudo-source
6 $Q \leftarrow N$
7 **for** k^* in $(1 : K^*)$ ▷ Reiterations

8 **do**
9 $\hat{\mathcal{T}}^0 \leftarrow \{\mathcal{T}_j\}_{j=1}^N$
10 **for** q in $(0 : Q - 1)$ **do**
11 $\mathcal{H} \leftarrow \{\}$
12 **Stage 1: Domain selection stage**
13 **for** \mathcal{T}_j in $\hat{\mathcal{T}}^q$ **do**
14 compute $H(\mathcal{T}_j)$
15 $\mathcal{H} \leftarrow \mathcal{H} \parallel H(\mathcal{T}_j)$
16 **end**
17 $\mathbb{D}^q \leftarrow \text{argmin}_j \mathcal{H}$
18 **Stage 2: Adaptation stage**
19 **for** k in $(1 : \frac{K}{K^*})$ ▷ Adaptation iterations
20 **do**
21 $\hat{B}_s^q \leftarrow (\mathbf{x}_{s,i}, y_{s,i})_{i=1}^{B_s} \sim \mathcal{S}^q$
22 $\hat{B}_t^q \leftarrow (\mathbf{x}_{t,i})_{i=1}^{B_t} \sim \mathcal{T}_{\mathbb{D}^q}$
23 $\hat{y} \leftarrow \text{softmax}(G_{mlp}(F(\mathbf{x})))$
24 $\bar{y} \leftarrow \text{softmax}(G_{gnn}(F(\mathbf{x})))$
25 $\hat{d} \leftarrow \text{sigmoid}(D(F(\mathbf{x})))$
26 update ψ by $\min_{\psi} \lambda_{adv} \ell_{adv}$
27 update θ, ϕ by $\min_{\theta, \phi} \ell_{ce}^{mlp} - \lambda_{adv} \ell_{adv}$
28 update $\theta, \varphi, \varphi'$ by
29 $\min_{\theta, \varphi, \varphi'} \lambda_{edge} \ell_{bce}^{edge} + \lambda_{node} \ell_{ce}^{node}$
30 **end**
31 **Stage 3: Pseudo-labeling stage**
32 $\mathcal{D}_t^{\mathbb{D}^q} \leftarrow \{\}$ **for** $\mathbf{x}_{t,j} \in \mathcal{T}_{\mathbb{D}^q}$ **do**
33 $w_j \leftarrow \max_{c \in n_c} p(\bar{y}_{t,j} = c | \mathbf{x}_{t,j})$
34 **if** $w_j > \tau$ **then**
35 $\mathcal{D}_t^{\mathbb{D}^q} \leftarrow$
36 $\mathcal{D}_t^{\mathbb{D}^q} \parallel \{(\mathbf{x}_{t,j}, \text{argmax}_{c \in n_c} p(\bar{y}_{t,j} =$
37 $c | \mathbf{x}_{t,j}))\}$
38 **end**
39 **end**
40 $\hat{\mathcal{S}}^{total} \leftarrow \hat{\mathcal{S}}^{total} \cup \mathcal{D}_t^{\mathbb{D}^q}$ ▷ Pseudo-source
41 $\hat{\mathcal{T}}^{q+1} = \hat{\mathcal{T}}^q \setminus \mathcal{T}_{\mathbb{D}^q}$
42 **end**
43 **end**

Step 3: Fine-tuning on the pseudo-source dataset using K' iterations

Network component	Architecture	Output
Feature extractor (F)	Transformer with bottleneck	$B \times 256$
MLP classifier (G_{mlp})	FC layer	$B \times n_c$
Edge network (f_{edge})	Conv(256,256,1), Conv(256,128,1), Conv(128,1,1)	$B \times B$
Node classifier (f_{node})	Conv(512, $2 \times n_c$, 1), Conv($2 \times n_c$, n_c , 1)	$B \times n_c$

Table 1. Network architecture assuming batch-size B . Conv(a,b,c) denote a convolutional filter with a input features, b output features, and kernel size $c \times c$.

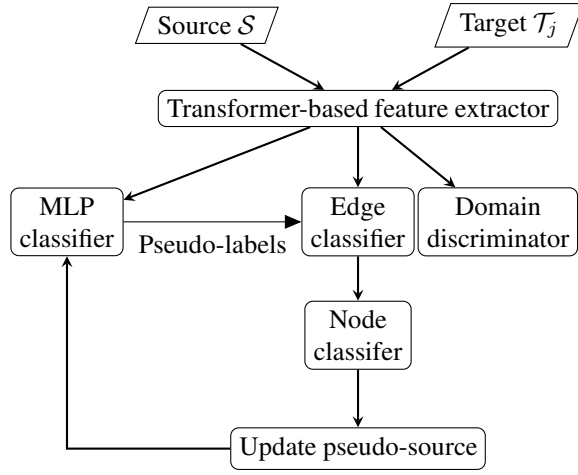


Fig. 1. Proposed method for adapting on a single target domain \mathcal{T}_j .

same label space and for each target sample their domain is known. Our goal is to learn predictor for the N target domains by using the labeled data \mathcal{S} and the unlabeled data \mathcal{T} .

3.1. Network structure

While any backbone feature extractor can be used, we use a Transformer-based feature extractor network F to extract the features from the input image, i.e., given an input \mathbf{x} , it generates the output $\mathbf{f} = F(\mathbf{x})$. Following this, features are fed to a MLP classifier G_{mlp} . Features are also fed to an edge-based network f_{edge} , the output of which is fed to f_{node} , a node classifier. The f_{edge} and f_{node} together form the G_{gnn} . Additionally, a domain discriminator network D is used. The parameters of networks F , D , G_{mlp} , f_{edge} , f_{node} are represented as $\theta, \psi, \phi, \varphi, \varphi'$, respectively. The network structure is shown in Table 1.

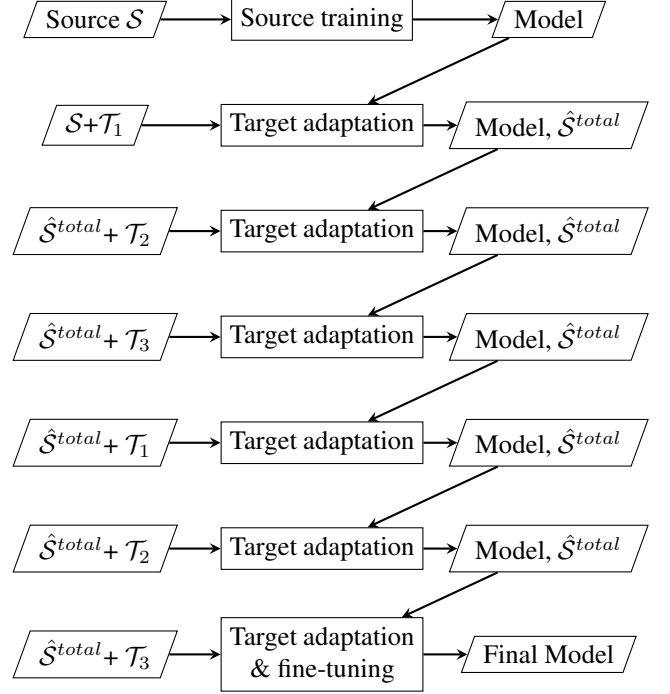


Fig. 2. Reiterative training approach assuming three target domains $\mathcal{T}_1, \mathcal{T}_2$, and \mathcal{T}_3 (in that order of closeness to the source domain) and two reiteration steps (i.e., $K^* = 2$). Model and pseudo-source $\hat{\mathcal{S}}^{total}$ is updated continuously.

3.2. Transformer-based feature extractor

We adopt the Transformer-based feature extractor from TransUNet [52] as a pre-trained feature extractor F . Instead of using a pure Transformer, a CNN-Transformer hybrid model is used. CNN is first applied to the input image to generate feature map and subsequently patch embedding is applied to 1×1 patches extracted from the CNN feature map to compute the input of the Transformer. Such hybrid CNN-Transformer encoder has shown good performance both in image segmentation [52] and domain adaptation [21]. For the CNN, we specifically employ ResNet-50 model [53]. The feature extractor backbone is pre-trained on ImageNet dataset [54].

3.3. Training on the source dataset

Before adapting on the targets \mathcal{T} , the source labeled samples $(\mathbf{x}_{s,i}, y_{s,i})_{i=1}^{n_s}$ are used to train the model F and G_{mlp} , thus updating the parameters θ and ϕ , respectively. While F consists of ResNet-Transformer model as described in Section 3.2, the G_{mlp} is a fully connected output layer consisting of n_c logits. Cross-entropy loss ℓ_{ce}^{mlp} computed from the source samples is used for training and the target samples are not used at this stage.

3.4. Pseudo-source

At each step of the target adaptation, we treat a selected set of samples $\hat{\mathcal{S}}^{total}$ as the samples for which we are confident about their labels. These samples are called pseudo-source ($\hat{\mathcal{S}}^{total}$) and is initialized with source samples \mathcal{S} after the step in Section 3.3. However target samples are slowly added to it, as explained in the following subsections.

3.5. Target adaptation

In this step the model performs feature adaptation on the target domains, one domain at a time, starting from the easiest domain and gradually moving to the more difficult ones. The easiest domain is defined as the domain closest to the source domain, which is measured by the uncertainty ($H(\mathcal{T}_j)$ for domain \mathcal{T}_j) in the target predictions with the source-trained model [16, 55].

Once one target domain to be processed is fixed, adaptation is performed for K iterations. In each iteration, some source samples ($\hat{\mathcal{B}}_s^q$) and some target samples ($\hat{\mathcal{B}}_t^q$) are drawn to form a minibatch. Each minibatch of images is fed to the feature extractor to obtain features corresponding to them and then fed to the G_{mlp} and G_{gnn} . The G_{gnn} consists of the edge network f_{edge} and the node classifier f_{node} . The G_{mlp} does not aggregate features from different samples, rather predict based on only the sample of interest. On the other hand GNN-based classifier aggregates the features of the samples in the batch. In other words, prediction from G_{gnn} not only accounts for a sample \mathbf{x} , rather also for the other samples in the minibatch. While this leads to potentially better context-aware learning paradigm, naively using it may lead to noisy feature degrading the classification performance. The MLP classifier and the GNN classifier capture different aspects, thus they are further exploited to provide feedback to each other, similar to co-teaching [25]. The output from the MLP head is obtained as:

$$\hat{y} \leftarrow \text{softmax}(G_{mlp}(F(\mathbf{x}))) \quad (1)$$

Similarly, the output from the GNN head is obtained as:

$$\bar{y} \leftarrow \text{softmax}(G_{gnn}(F(\mathbf{x}))) \quad (2)$$

The G_{mlp} and f_{node} of G_{gnn} is trained with cross-entropy loss ℓ_{ce}^{mlp} and ℓ_{ce}^{edge} , respectively, computed over the source/pseudo-source samples.

Feedback from MLP to GNN: For edge network f_{edge} to learn the pairwise similarity between samples, a target matrix $\hat{\mathcal{A}}^{tar}$ is formed such that an element \hat{a}^{tar} in $\hat{\mathcal{A}}^{tar}$ is 1 if the labels of i -th and j -th sample are same. While label information is known from the source samples ($\hat{\mathcal{B}}_s^q$), they are not known for the target samples ($\hat{\mathcal{B}}_t^q$). Thus, pseudo-labels of target samples are formed using prediction of G_{mlp} . In this way G_{mlp} teaches G_{gnn} . A (binary-cross-entropy) edge loss

between elements of affinity matrix $\hat{\mathcal{A}}$ (produced by f_{edge}) and the target matrix $\hat{\mathcal{A}}^{tar}$ is computed as ℓ_{bce}^{edge} .

Feedback from GNN to MLP: At the end of processing each target domain, a score w_j is assigned to each sample $\mathbf{x}_{t,j}$ in the target domain as:

$$w_j \leftarrow \max_{c \in n_c} p(\bar{y}_{t,j} = c | \mathbf{x}_{t,j}) \quad (3)$$

w_j indicates the confidence of prediction of G_{gnn} for the sample j . If w_j is greater than a score τ , then this sample is appended to the list of pseudo-labeled samples $\hat{\mathcal{S}}^{total}$ that are used while processing the subsequent target domains. In this way, the G_{gnn} creates a set of context-aware pseudo-samples after processing each target domain, thus enabling more effective learning of G_{mlp} .

Domain discriminator: In addition to the MLP and GNN based networks, a domain discriminator D is used to predict the domain of the samples [8, 28]. The output from this is obtained as:

$$\hat{d} \leftarrow \text{sigmoid}(D(F(\mathbf{x}))) \quad (4)$$

The domain discriminator in conjunction with a gradient reversal layer (GRL) is trained with an adversarial loss ℓ_{adv} . This further pushes the feature extractor to learn features such that the source and different target features appear as if they are coming from the same distribution.

The target adaptation processing assuming a single target is shown in Figure 1.

3.6. Reiterative target adaptation

The target adaptation, as explained in Section 3.5 makes only one pass through the easiest to the most difficult domain (with K training iterations for each domain). The model will not be sufficiently adapted to the target domains if the chosen value of K is small. However, if value of K is big, the softmax values produced by the model may be large even for the samples for which the model is not confident [26]. This may cause erroneous samples selected in pseudo-source $\hat{\mathcal{S}}^{total}$. To circumnavigate this problem, we propose to make multiple (K^*) passes (we call it reiteration) through each domain.

In more details, if there are only three target domains \mathcal{T}_1 , \mathcal{T}_2 , and \mathcal{T}_3 (in that order of difficulty), the target adaptation in Section 3.5 processes it only once in the order \mathcal{T}_1 , \mathcal{T}_2 , and \mathcal{T}_3 . Instead, using the reiterative strategy, if $K^* = 2$, proposed method processes the target domains in the order \mathcal{T}_1 , \mathcal{T}_2 , \mathcal{T}_3 , \mathcal{T}_1 , \mathcal{T}_2 , and \mathcal{T}_3 . Reiterative approach is further illustrated in Figure 2.

We also propose to scale down the number of training iterations (per reiteration) by a factor of K^* . In this way, proposed method with K^* reiteration passes uses the same number of iterations as original D-CGCT with K adaptation iterations per target domain. By only iterating K/K^* times per target domain in a reiteration, the target adaptation process does not push itself too hard, thus avoiding to produce high

softmax values for low-confident samples. On the other hand, with increasing reiterative passes, the adaptation process unfolds slowly, however in a more effective manner.

3.7. Emphasizing source samples

We furthermore postulate that more source samples in a mini-batch can lead to more effective target adaptation. In other words, instead of setting $B_s = B_t = B$, we propose to set $B_s > B_t$. Such a modification does not affect the number of training iterations. Moreover, $B_s + B_t$ can be kept fixed by simply decreasing B_t while increasing B_s .

The proposed method is detailed in Algorithm 1.

3.8. Using trained model for inference

Once the proposed MLP-GNN dual head model is trained, either head can be used during inference to determine the class of a target test sample. However, as noted in [16], the GNN head requires mini-batch of samples, that may not be available during real-world inference. Hence, once trained, it is more practical to use the MLP head for inference.

4. EXPERIMENTAL VALIDATION

4.1. Datasets

We conducted experiments on standard three domain adaptation datasets.

Office-Home dataset contains 4 domains (Art, Clipart, Product, Real) and 65 classes [56].

Office-31 dataset contains 3 domains (Amazon, DSLR, Webcam) and 31 classes [57].

DomainNet dataset contains 6 domains and 345 classes [13]. Compared to the other two datasets, this one is very large scale containing 0.6 million images. The 6 domains are Real (R), Painting (P), Sketch (S), Clipart (C), Infograph (I), Quickdraw (Q).

4.2. Evaluation protocol and settings

Like previous works on MTDA [16], we use the classification accuracy to evaluate the performance of proposed method. The performance for a given source is given by setting the remaining domains as target domains and averaging the accuracy on all the target domains.

For sake of fairness of comparison, we use the the same set of hyperparameters as reported in [16]. In addition to D-CGCT [16], comparison is shown to MT-MTDA [15] and Conditional Adversarial Domain Adaptation (CDAN) [28] along with domain-aware curriculum learning (DCL), i.e., CDAN+DCL, as shown in [16]. For DomainNet, comparison is also provided to HGAN [38].

k	Corr.	Incorr.	Δ corr.	Δ incorr.
1	2518	338	-	-
500	2798	389	280	51
1000	2868	445	70	56

Table 2. Variation of correct and incorrect pseudo-samples as adaptation iteration (k) progresses. The last two columns indicate the change in number of correct and incorrect pseudo-samples. The result is shown Office-Home dataset for Product as target, using Art as source.

K^*	1	3	5	10	20
Acc.	70.5	72.4	73.4	73.6	72.8

Table 3. The performance variation w.r.t. reiteration numbers (K^*) on Office-Home dataset, source - Art, target - rest. The target accuracy is averaged over all the target domains. We observe that as K^* is increased, target classification accuracy either improves or remains similar. The best result is obtained for $K^* = 10$.

4.3. Analyses on Office-Home dataset

We perform several analyses and ablation studies on the Office-Home dataset. These experiments simply use ResNet-50 (not Transformer) backbone as in [16], unless otherwise stated.

We hypothesized in Section 3.6 that attempting to adapt model on a target for too many iterations (big K) may instead produce large softmax values even for samples for which model is not confident, thus yielding unreliable pseudo-samples. To verify this, we show the progress of pseudo-sample selection for Art as source and Product as target in Table 2. It is evident that for the first few hundred iterations, more correct samples are added. However as training is prolonged, more and more incorrect samples exceed the softmax threshold and are added to pseudo-source. This validates our hypothesis that attempting to prolong training may impact the adaptation process negatively.

Taking Art as source and rest as target, we vary the number of reiteration (K^*), as explained in Section 3.6. In this experiment, we use $B_s = 32, B_t = 32$. Here, $K^* = 1$ is equivalent to using D-CGCT. We observe that the target accuracy improves as K^* increases. Best target accuracy is obtained at $K^* = 10$. Following [16], we used $K = 10000$. Thus, $K^* = 10$ implies decomposing the adaptation process into 10 reiterations of $\frac{K}{K^*} = 1000$ iterations each. In the rest of the experiments related to Office-Home dataset, $K^* = 10$ is used.

After each reiteration, some new target samples are added to the pseudo-source \hat{S}^{total} . Taking Art as source and rest as target, we show this process in Table 4 for $K^* = 10$. We observe that the reiterative process allows to gradually ingest the pseudo-samples, more at the first reiteration and gradually

k^*	Real	Product	Clipart	Target Acc.
1	2788	2912	2058	65.6
2	769	810	843	70.0
3	280	255	420	71.3
4	137	162	250	72.2
5	68	82	160	72.8
6	53	59	106	73.0
7	35	30	80	73.4
8	26	20	55	73.4
9	20	17	44	73.5
10	11	11	32	73.6

Table 4. Column 2-4 indicates the number of pseudo-samples selected from the target domains after each re-iteration k^* (Office-Home dataset, taking Art as source). Note that total reiteration is fixed as $K^* = 10$. Final column indicates the average target classification accuracy after each reiteration

B_s, B_t	32,32	48,16	48,32
Target Acc.	73.6	73.7	75.1

Table 5. The performance variation w.r.t. source and target samples in a minibatch (B_s, B_t) on Office-Home dataset, source - Art, target - rest. The target accuracy is averaged over all the target domains.

less in the subsequent reiterations. E.g., for the target domain Real, 2788 samples are added to pseudo-source at the first reiteration, followed by 769 and 280 new samples added to the pseudo-source in the following two reiterations and so on. A gradual improvement in average target classification accuracy is observed over the reiterations.

We hypothesized in Section 3.7 that using more source samples in the training minibatch may improve the target adaptation. To examine this, we vary value of B_s and B_t , as shown in Table 5 taking Art as source and rest as target. Among the three compared settings, $B_s = 48, B_t = 32$ obtains the best result. Even with $B_s = 48$ and $B_t = 16$, improvement is observed over $B_s = B_t = 32$. Though $B_s = 48, B_t = 32$ is better, we use $B_s = 48, B_t = 16$ combination for subsequent experiments, to keep $B_s + B_t$ value same as in [16].

We further show in Table 6 that the correctly chosen pseudo-samples increase after employing reiterative strategy and using more source samples in minibatch.

Using Transformer as the backbone feature extractor further improves the performance of the proposed method, as shown in Table 7.

Finally we show that the proposed reiterative strategy outperforms D-CGCT [16] in most cases irrespective of the feature extractor backbone. This is shown on all 4 domains (Art, Clipart, Product, Real) as source, while treating other three as target. Performance improvement is consistent for ResNet-

K^*, B_s, B_t	Real	Product	Clipart
1,32,32	2969	3047	1971
10,48,16	3537	3480	2580

Table 6. Correct pseudo-sample at last iteration. Dataset: Office-Home, Source: Art, target: rest.

k^*	B_s	B_t	Backbone	Acc.
1	32	32	ResNet-50	70.5
10	32	32	ResNet-50	73.6
10	48	16	ResNet-50	73.7
10	48	16	Transformer	80.8

Table 7. Variation of 4 components of the proposed method (k^*, B_s, B_t , and backbone) on Office-Home dataset, source: Art, target: rest.

18, ResNet-50, and Transformer (except one case), as shown in Table 8.

Henceforth, the proposed method is shown with Transformer-based feature extractor, as detailed in Section 3.2. Accuracy reported for D-CGCT is however from [16], with architecture of their choice.

4.4. Quantitative comparisons

Office-Home: The proposed method outperforms D-CGCT (and other compared methods) for all four domains. The performance improvement is quite prominent, Art (10.3%), Clipart (10.2%), Product (14.7%), and Real (7.6%). This may be attributed to both use of Transformer as backbone feature extractor and the reiterative training strategy. The performance improvement is almost uniform for all domains, except for the Real domain. On average it outperforms D-CGCT by 10.7%. The quantitative result of Office-Home dataset is shown in Table 9.

Office-31: Originally in [16], target adaptation iterations K is set as 3000 for Office-31 dataset. We set number of reiterations $K^* = 3$ to keep $\frac{K}{K^*} = 1000$, as in Office-Home.

The proposed method outperforms D-CGCT for DSLR (3.4%) and Webcam (2.8%) and obtains similar performance for Amazon. Remarkably, proposed method shows the least improvement for Amazon as source, which has the most number of images in Office-31 dataset. This indicates a possibility that the improvement brought by the proposed method diminishes if there are abundant images in the labeled source domain, which is often not the case in practice. The quantitative result of the Office-31 dataset is shown in Table 10.

DomainNet: Like other two datasets, we chose K^* such that $\frac{K}{K^*} = 1000$. The quantitative result for the different source \rightarrow target combinations are shown in Table 11, following the format in [38]. Performance improves over D-CGCT in most cases, e.g., $R \rightarrow S$ (10.2%), $R \rightarrow C$ (8.1%), $R \rightarrow I$ (5.6%), $R \rightarrow P$ (5.4%), $P \rightarrow S$ (2.2%) and $P \rightarrow I$ (2.5%).

Method	Art	Clip.	Prod.	Real
D-CGCT (ResNet-18)	61.4	60.7	57.3	63.8
Proposed (ResNet-18)	64.9	65.4	61.8	66.7
D-CGCT (ResNet-50)	70.5	71.6	66.0	71.2
Proposed (ResNet-50)	73.7	76.0	68.7	72.7
D-CGCT (Transformer)	77.0	78.5	77.9	80.9
Proposed (Transformer)	80.8	81.8	80.7	78.8

Table 8. The performance comparison on the Office-Home dataset when using different architectures as backbone.

Method	Art	Clipart	Product	Real
MT-MTDA	64.6	66.4	59.2	67.1
CDAN+DCL	63.0	66.3	60.0	67.0
D-CGCT	70.5	71.6	66.0	71.2
Proposed	80.8	81.8	80.7	78.8

Table 9. The performance comparison on the Office-Home dataset. The classification accuracy is reported for each source and the rest set as target, with each source domain being indicated in the columns.

5. LIMITATIONS

The proposed method requires data from the source domain while adapting the model to target. This may potentially limit its practical application and needs to be addressed in the future by modifying the proposed method for source-free domain adaptation [58]. The method does not account for possible presence of open sets [59, 60]. While use of a heavier backbone (Transformer) may also be considered a limitation of the proposed method, it is shown in Section 4.3 that proposed method outperforms other methods even for lighter architectures.

6. CONCLUSION

While single-source single-target domain adaptation has been long studied in the literature, its practical applications are limited. Thus domain adaptation is moving beyond this simple setting towards more practical and complex settings, e.g., multi-target adaptation. Our work takes forward multi-target adaptation by exploiting Transformer along with graph neural network. The proposed reiterative adaptation strategy enhances the target adaptation performance by enabling the network to select more accurate pseudo-samples. The proposed method consistently improves result for Office-Home and Office-31 datasets and almost always for the DomainNet dataset. In the future we plan to extend the method for multi-source multi-target adaptation and source-free adaptation.

Method	Amazon	DSLRL	Webcam
MT-MTDA	87.9	83.7	84.0
CDAN+DCL	92.6	82.5	84.7
D-CGCT	93.4	86.0	87.1
Proposed	93.4	89.4	89.9

Table 10. The performance comparison on the Office-31 dataset. The classification accuracy is reported for each source and the rest set as target, with each source domain being indicated in the columns.

7. REFERENCES

- [1] Y. LeCun, Y. Bengio, and G. Hinton, “Deep learning,” *nature*, vol. 521, no. 7553, pp. 436–444, 2015.
- [2] I. Goodfellow, Y. Bengio, and A. Courville, *Deep learning*. MIT press, 2016.
- [3] O. Ronneberger, P. Fischer, and T. Brox, “U-net: Convolutional networks for biomedical image segmentation,” in *International Conference on Medical image computing and computer-assisted intervention*, pp. 234–241, Springer, 2015.
- [4] S. Saha, S. Sudhakaran, B. Banerjee, and S. Pendurkar, “Semantic guided deep unsupervised image segmentation,” in *International Conference on Image Analysis and Processing*, pp. 499–510, Springer, 2019.
- [5] X. Guo, X. Liu, E. Zhu, and J. Yin, “Deep clustering with convolutional autoencoders,” in *International Conference on Neural Information Processing*, pp. 373–382, Springer, 2017.
- [6] Y. Zhang, T. Liu, M. Long, and M. Jordan, “Bridging theory and algorithm for domain adaptation,” in *International Conference on Machine Learning*, pp. 7404–7413, PMLR, 2019.
- [7] M. Long, H. Zhu, J. Wang, and M. I. Jordan, “Unsupervised domain adaptation with residual transfer networks,” *arXiv preprint arXiv:1602.04433*, 2016.
- [8] Y. Ganin and V. Lempitsky, “Unsupervised domain adaptation by backpropagation,” in *International conference on machine learning*, pp. 1180–1189, PMLR, 2015.
- [9] W. Hong, Z. Wang, M. Yang, and J. Yuan, “Conditional generative adversarial network for structured domain adaptation,” in *Proceedings of the IEEE Conference on Computer Vision and Pattern Recognition*, pp. 1335–1344, 2018.

Method	R→S	R→C	R→I	R→P	P→S	P→R	P→C	P→I
HGAN	34.3	43.2	17.8	43.4	35.7	52.3	35.9	15.6
CDAN+DCL	45.2	58.0	23.7	54.0	45.0	61.5	50.7	20.3
D-CGCT	48.4	59.6	25.3	55.6	45.3	58.2	51.0	21.7
Proposed	58.6	67.7	30.9	61.0	47.5	55.9	48.6	24.2

Table 11. The performance comparison on the DomainNet dataset. Domains are Real (R), Painting (P), Sketch (S), Clipart (C), and Infograph (I). R→S indices Real as source and Sketch as target, similarly for other cases.

- [10] K. Bousmalis, N. Silberman, D. Dohan, D. Erhan, and D. Krishnan, “Unsupervised pixel-level domain adaptation with generative adversarial networks,” in *Proceedings of the IEEE Conference on Computer Vision and Pattern Recognition*, pp. 3722–3731, 2017.
- [11] E. Tzeng, J. Hoffman, K. Saenko, and T. Darrell, “Adversarial discriminative domain adaptation,” in *Proceedings of the IEEE Conference on Computer Vision and Pattern Recognition*, pp. 7167–7176, 2017.
- [12] M. Long, J. Wang, G. Ding, J. Sun, and P. S. Yu, “Transfer joint matching for unsupervised domain adaptation,” in *Proceedings of the IEEE conference on computer vision and pattern recognition*, pp. 1410–1417, 2014.
- [13] X. Peng, Q. Bai, X. Xia, Z. Huang, K. Saenko, and B. Wang, “Moment matching for multi-source domain adaptation,” in *Proceedings of the IEEE/CVF International Conference on Computer Vision*, pp. 1406–1415, 2019.
- [14] Y. Li, N. Wang, J. Shi, X. Hou, and J. Liu, “Adaptive batch normalization for practical domain adaptation,” *Pattern Recognition*, vol. 80, pp. 109–117, 2018.
- [15] L. T. Nguyen-Meidine, A. Belal, M. Kiran, J. Dolz, L.-A. Blais-Morin, and E. Granger, “Unsupervised multi-target domain adaptation through knowledge distillation,” in *Proceedings of the IEEE/CVF Winter Conference on Applications of Computer Vision*, pp. 1339–1347, 2021.
- [16] S. Roy, E. Krivosheev, Z. Zhong, N. Sebe, and E. Ricci, “Curriculum graph co-teaching for multi-target domain adaptation,” in *Proceedings of the IEEE/CVF Conference on Computer Vision and Pattern Recognition*, pp. 5351–5360, 2021.
- [17] K. Han, Y. Wang, H. Chen, X. Chen, J. Guo, Z. Liu, Y. Tang, A. Xiao, C. Xu, Y. Xu, *et al.*, “A survey on visual transformer,” *arXiv preprint arXiv:2012.12556*, 2020.
- [18] A. Dosovitskiy, L. Beyer, A. Kolesnikov, D. Weissenborn, X. Zhai, T. Unterthiner, M. Dehghani, M. Minderer, G. Heigold, S. Gelly, *et al.*, “An image is worth 16x16 words: Transformers for image recognition at scale,” *arXiv preprint arXiv:2010.11929*, 2020.
- [19] D. Malpure, O. Litake, and R. Ingle, “Investigating transfer learning capabilities of vision transformers and cnns by fine-tuning a single trainable block,” *arXiv preprint arXiv:2110.05270*, 2021.
- [20] L. T. Duong, N. H. Le, T. B. Tran, V. M. Ngo, and P. T. Nguyen, “Detection of tuberculosis from chest x-ray images: Boosting the performance with vision transformer and transfer learning,” *Expert Systems with Applications*, vol. 184, p. 115519, 2021.
- [21] G. Yang, H. Tang, Z. Zhong, M. Ding, L. Shao, N. Sebe, and E. Ricci, “Transformer-based source-free domain adaptation,” *arXiv preprint arXiv:2105.14138*, 2021.
- [22] J. Zhou, G. Cui, S. Hu, Z. Zhang, C. Yang, Z. Liu, L. Wang, C. Li, and M. Sun, “Graph neural networks: A review of methods and applications,” *AI Open*, vol. 1, pp. 57–81, 2020.
- [23] L. Jiang, D. Meng, Q. Zhao, S. Shan, and A. G. Hauptmann, “Self-paced curriculum learning,” in *Twenty-Ninth AAAI Conference on Artificial Intelligence*, 2015.
- [24] A. Graves, M. G. Bellemare, J. Menick, R. Munos, and K. Kavukcuoglu, “Automated curriculum learning for neural networks,” in *international Conference on Machine Learning*, pp. 1311–1320, PMLR, 2017.
- [25] B. Han, Q. Yao, X. Yu, G. Niu, M. Xu, W. Hu, I. Tsang, and M. Sugiyama, “Co-teaching: Robust training of deep neural networks with extremely noisy labels,” *arXiv preprint arXiv:1804.06872*, 2018.
- [26] C. Guo, G. Pleiss, Y. Sun, and K. Q. Weinberger, “On calibration of modern neural networks,” in *International Conference on Machine Learning*, pp. 1321–1330, PMLR, 2017.
- [27] M. Hein, M. Andriushchenko, and J. Bitterwolf, “Why relu networks yield high-confidence predictions far away from the training data and how to mitigate the problem,” in *Proceedings of the IEEE/CVF Conference on Computer Vision and Pattern Recognition*, pp. 41–50, 2019.

- [28] M. Long, Z. Cao, J. Wang, and M. I. Jordan, “Conditional adversarial domain adaptation,” *arXiv preprint arXiv:1705.10667*, 2017.
- [29] P. Panareda Busto and J. Gall, “Open set domain adaptation,” in *Proceedings of the IEEE International Conference on Computer Vision*, pp. 754–763, 2017.
- [30] K. Saito, S. Yamamoto, Y. Ushiku, and T. Harada, “Open set domain adaptation by backpropagation,” in *Proceedings of the European Conference on Computer Vision (ECCV)*, pp. 153–168, 2018.
- [31] T. Jing, H. Liu, and Z. Ding, “Towards novel target discovery through open-set domain adaptation,” *arXiv preprint arXiv:2105.02432*, 2021.
- [32] S. Sun, H. Shi, and Y. Wu, “A survey of multi-source domain adaptation,” *Information Fusion*, vol. 24, pp. 84–92, 2015.
- [33] K. Zhang, M. Gong, and B. Schölkopf, “Multi-source domain adaptation: A causal view,” in *Twenty-ninth AAAI conference on artificial intelligence*, 2015.
- [34] R. Gong, D. Dai, Y. Chen, W. Li, and L. Van Gool, “mdalu: Multi-source domain adaptation and label unification with partial datasets,” in *Proceedings of the IEEE/CVF International Conference on Computer Vision*, pp. 8876–8885, 2021.
- [35] H. Yu, M. Hu, and S. Chen, “Multi-target unsupervised domain adaptation without exactly shared categories,” *arXiv preprint arXiv:1809.00852*, 2018.
- [36] T. Isobe, X. Jia, S. Chen, J. He, Y. Shi, J. Liu, H. Lu, and S. Wang, “Multi-target domain adaptation with collaborative consistency learning,” in *Proceedings of the IEEE/CVF Conference on Computer Vision and Pattern Recognition*, pp. 8187–8196, 2021.
- [37] B. Gholami, P. Sahu, O. Rudovic, K. Bousmalis, and V. Pavlovic, “Unsupervised multi-target domain adaptation: An information theoretic approach,” *IEEE Transactions on Image Processing*, vol. 29, pp. 3993–4002, 2020.
- [38] X. Yang, C. Deng, T. Liu, and D. Tao, “Heterogeneous graph attention network for unsupervised multiple-target domain adaptation,” *IEEE Transactions on Pattern Analysis and Machine Intelligence*, 2020.
- [39] Z. Chen, J. Zhuang, X. Liang, and L. Lin, “Blending-target domain adaptation by adversarial meta-adaptation networks,” in *Proceedings of the IEEE/CVF Conference on Computer Vision and Pattern Recognition*, pp. 2248–2257, 2019.
- [40] A. Rosenfeld and J. K. Tsotsos, “Incremental learning through deep adaptation,” *IEEE Transactions on Pattern Analysis and Machine Intelligence*, vol. 42, no. 3, pp. 651–663, 2018.
- [41] M. Mancini, S. R. Buló, B. Caputo, and E. Ricci, “Adagraph: Unifying predictive and continuous domain adaptation through graphs,” in *Proceedings of the IEEE/CVF Conference on Computer Vision and Pattern Recognition*, pp. 6568–6577, 2019.
- [42] M. Wulfmeier, A. Bewley, and I. Posner, “Incremental adversarial domain adaptation for continually changing environments,” in *2018 IEEE International conference on robotics and automation (ICRA)*, pp. 4489–4495, IEEE, 2018.
- [43] T. N. Kipf and M. Welling, “Semi-supervised classification with graph convolutional networks,” *arXiv preprint arXiv:1609.02907*, 2016.
- [44] Y. Luo, Z. Wang, Z. Huang, and M. Baktashmotlagh, “Progressive graph learning for open-set domain adaptation,” in *International Conference on Machine Learning*, pp. 6468–6478, PMLR, 2020.
- [45] H. Touvron, M. Cord, M. Douze, F. Massa, A. Sablayrolles, and H. Jégou, “Training data-efficient image transformers & distillation through attention,” in *International Conference on Machine Learning*, pp. 10347–10357, PMLR, 2021.
- [46] H. Wu, B. Xiao, N. Codella, M. Liu, X. Dai, L. Yuan, and L. Zhang, “Cvt: Introducing convolutions to vision transformers,” *arXiv preprint arXiv:2103.15808*, 2021.
- [47] A. Hassani, S. Walton, N. Shah, A. Abuduweili, J. Li, and H. Shi, “Escaping the big data paradigm with compact transformers,” *arXiv preprint arXiv:2104.05704*, 2021.
- [48] Y. Li, K. Zhang, J. Cao, R. Timofte, and L. Van Gool, “Localvit: Bringing locality to vision transformers,” *arXiv preprint arXiv:2104.05707*, 2021.
- [49] K. Lee, H. Chang, L. Jiang, H. Zhang, Z. Tu, and C. Liu, “Vitgan: Training gans with vision transformers,” *arXiv preprint arXiv:2107.04589*, 2021.
- [50] J. Beal, E. Kim, E. Tzeng, D. H. Park, A. Zhai, and D. Kislyuk, “Toward transformer-based object detection,” *arXiv preprint arXiv:2012.09958*, 2020.
- [51] S. Wu, T. Wu, F. Lin, S. Tian, and G. Guo, “Fully transformer networks for semantic image segmentation,” *arXiv preprint arXiv:2106.04108*, 2021.

- [52] J. Chen, Y. Lu, Q. Yu, X. Luo, E. Adeli, Y. Wang, L. Lu, A. L. Yuille, and Y. Zhou, “Transunet: Transformers make strong encoders for medical image segmentation,” *arXiv preprint arXiv:2102.04306*, 2021.
- [53] K. He, X. Zhang, S. Ren, and J. Sun, “Deep residual learning for image recognition,” in *Proceedings of the IEEE conference on computer vision and pattern recognition*, pp. 770–778, 2016.
- [54] J. Deng, W. Dong, R. Socher, L.-J. Li, K. Li, and L. Fei-Fei, “Imagenet: A large-scale hierarchical image database,” in *2009 IEEE conference on computer vision and pattern recognition*, pp. 248–255, Ieee, 2009.
- [55] Y. Gal, “Uncertainty in deep learning,” 2016.
- [56] H. Venkateswara, J. Eusebio, S. Chakraborty, and S. Panchanathan, “Deep hashing network for unsupervised domain adaptation,” in *Proceedings of the IEEE conference on computer vision and pattern recognition*, pp. 5018–5027, 2017.
- [57] K. Saenko, B. Kulis, M. Fritz, and T. Darrell, “Adapting visual category models to new domains,” in *European conference on computer vision*, pp. 213–226, Springer, 2010.
- [58] J. N. Kundu, A. Kulkarni, A. Singh, V. Jampani, and R. V. Babu, “Generalize then adapt: Source-free domain adaptive semantic segmentation,” in *Proceedings of the IEEE/CVF International Conference on Computer Vision*, pp. 7046–7056, 2021.
- [59] X. Ma, J. Gao, and C. Xu, “Active universal domain adaptation,” in *Proceedings of the IEEE/CVF International Conference on Computer Vision*, pp. 8968–8977, 2021.
- [60] H. Xia, H. Zhao, and Z. Ding, “Adaptive adversarial network for source-free domain adaptation,” in *Proceedings of the IEEE/CVF International Conference on Computer Vision*, pp. 9010–9019, 2021.